

Effect of Heavy Atoms on the Thermal Stability of α -Amylase from *Aspergillus oryzae*

Michihiro Sugahara*, Michiyo Takehira, Katsuhide Yutani

RIKEN SPring-8 Center, Sayo, Hyogo, Japan

Abstract

Currently, there are no versatile and established methods for improving stability of proteins. In an entirely different approach from conventional techniques such as mutagenesis, we attempted to enhance enzyme stability of α -amylase from *Aspergillus oryzae* using a heavy-atom derivatization technique. We evaluated changes in stability using differential scanning calorimetry (DSC). Candidate heavy atoms were identified using the Heavy-Atom Database System *HATODAS*, a Web-based tool designed to assist in heavy-atom derivatization of proteins for X-ray crystallography. The denaturation temperature of α -amylase derivatized with gadolinium (Gd) or samarium (Sm) ions increased by 6.2 or 5.7°C, respectively, compared to that of the native protein (60.6°C). The binding of six Gd ions was confirmed by X-ray crystallography of the enzyme at 1.5 Å resolution. DSC and dynamic light-scattering data revealed a correlation between stability and the aggregation state upon addition of Gd ions. These results show that *HATODAS* search is an effective tool for selecting heavy atoms for stabilization of this protein.

Citation: Sugahara M, Takehira M, Yutani K (2013) Effect of Heavy Atoms on the Thermal Stability of α -Amylase from *Aspergillus oryzae*. PLoS ONE 8(2): e57432. doi:10.1371/journal.pone.0057432

Editor: Israel Silman, Weizmann Institute of Science, Israel

Received: September 10, 2012; **Accepted:** January 22, 2013; **Published:** February 25, 2013

Copyright: © 2013 Sugahara et al. This is an open-access article distributed under the terms of the Creative Commons Attribution License, which permits unrestricted use, distribution, and reproduction in any medium, provided the original author and source are credited.

Funding: This work was supported in part by a '2010 Incentive Research Grant' from Hyogo Science and Technology Association (No. 22S022) and by a 'Grant in Aid for Scientific Research' from Japan Society for the Promotion of Science (KAKENHI No. 22770116). The funders had no role in study design, data collection and analysis, decision to publish, or preparation of the manuscript.

Competing Interests: The authors have declared that no competing interests exist.

* E-mail: msuga@spring8.or.jp

Introduction

Enzymes are currently used in many different industrial products and processes [1]. To enhance thermal stability of highly useful enzymes for industrial applications, protein-engineering techniques such as site-directed mutagenesis, random mutagenesis, recombination, and directed-evolution techniques have been successfully employed for various proteins [2,3]. To date, most stability improvements have been based on the introduction of point mutations into proteins. In general, however, there are no established methods that can be used to predict the effect of mutations on thermal stability, because even single amino-acid substitutions affect various stabilization factors depending on the surrounding environment, substituted residues, and structural changes due to the mutations [4–6]. Therefore, a versatile and simple method for thermal stabilization of enzymes is required.

As well as the site directed mutagenesis, techniques for protein stability by using additives such as covalent cross-linkers and ligands have been well studied since early times. The covalent cross-linking technique by bifunctional chemical modification reagents [7,8] as an additive has been successfully used to enhance the stability of proteins [9]. The cross-linking in proteins reduces the configurational backbone chain entropy of the unfolded polypeptide, resulting in increase in conformational stability [10–12]. On the other hand, the binding of ligand increases the stability of proteins in response to Schellman's binding theory [13,14]. The stabilization mechanism can be explained stoichiometrically by the shift of the folding-unfolding equilibrium toward the folded state caused by the higher affinity of ligand to the folded state [15]. Thus these techniques using the additives have the

advantages of being simple and quick, and are useful for enhancing protein stability efficiently.

Metal ions that bind with high affinity to specific sites often stabilize the conformation of proteins [16–21]. In protein X-ray crystallography, experimental phasing from heavy atom-derivatized crystals is a major technique in structure determination [22]. The identification of heavy atoms that bind proteins can be useful both for improving crystallization success rates and in some cases for enhancing the thermal stability of these proteins [23]. However, determination of candidate heavy atoms is laborious and time-consuming. Recently, to facilitate the heavy-atom derivatization process, we developed the Heavy-Atom Database System (*HATODAS*, <http://hatodas.harima.riken.jp>), which suggests candidate heavy-atom reagents for a target protein based on a search against a database of known heavy atom-liganded proteins, using the amino-acid sequence and crystallization conditions as the query terms [24,25]. We believe that *HATODAS* search could also contribute to the efficient selection of candidate heavy atoms for use in protein stabilization using the derivatization technique.

Here we present such a method, which utilizes derivatization with heavy atoms identified through *HATODAS* search. This study was designed to investigate whether there is a relationship between heavy-atom-derivatized protein and its conformational stability; to date, there has been no detailed study of the effect of heavy atoms on protein stability. To elucidate thermal behavior of a derivatized protein, we used differential scanning calorimetry (DSC) to investigate the stability of *Aspergillus oryzae* α -amylase (Ao α -amylase) containing heavy atoms. This enzyme catalyzes the

hydrolysis of the α -1,4 glycosidic linkages in raw and soluble starches, and is used in numerous industrial applications for starch conversion in value-added products. The stability of Ao α -amylase containing heavy atoms was evaluated over a wide range of concentrations by heat denaturation, and the structures of the derivatized proteins were determined by X-ray crystallography. We also discuss the thermostabilization mechanism of heavy atom-derivatized Ao α -amylase.

Results and Discussion

Heavy-atom selection for thermostabilization

Six candidate heavy atoms for thermostabilization of Ao α -amylase were selected using the program *HATODAS*. The order of the top six was (1) mercury (Hg), (2) bromine (Br), (3) platinum (Pt), (4) samarium (Sm), (5) lead (Pb), and (6) thallium (Tl).

Because heavy atoms sometimes act as inhibitors, we first investigated whether derivatized proteins retained their enzymatic activity. We examined the activity of Ao α -amylase with each heavy atom at room temperature; digestion of starch was assayed by monitoring the disappearance of the starch-iodine color. In the presence of the six heavy atoms, activity was preserved, indicating that none of these heavy atoms is a potent inhibitor of the enzyme. In general, heavy atoms bind to characteristic residues: Hg, Au, and Ag tend to bind to Cys or His; Pt binds to Met or His; and Pb and lanthanides bind to Asp or Glu [25]. To avoid inactivation of the enzyme, heavy atoms should be selected based on the types of amino acids constituting the protein active site.

To further characterize these heavy atoms, we examined the stability of Ao α -amylase derivatized with each candidate. Solutions of each derivatized Ao α -amylase were incubated in a water bath at $\sim 70^\circ\text{C}$ for 5 min, and the remaining activity was evaluated at room temperature. Only Sm, the fourth of six candidate atoms in terms of stabilization potential, had a significant effect on thermal stability of the enzyme; the other samples did not exhibit enzymatic activity after heat treatment. Although we confirmed that the Ao α -amylase crystals had been successfully derivatized with Hg ion, which *HATODAS* predicted would yield the greatest stabilization, this ion did not in fact stabilize this protein. In any case, use of Hg ions should be avoided because the accumulation of Hg from industrial uses poses serious environmental problems.

Based on these findings, we excluded heavy atoms other than Sm from further characterization, since they did not enhance the stability of this enzyme. However, because structure determination of the Sm-binding protein was not successful (see Materials and Methods), we performed additional *HATODAS* searches for lanthanide ions as a substitute for Sm, resulting in the identification of gadolinium (Gd) as a new candidate. Activity evaluation after heat treatment revealed that derivatization with Gd ion yielded heat-stabilization similar to that observed with Sm ion. Furthermore, we were able to successfully determine the crystal structure of Gd-derivatized protein. Therefore, we elected to further characterize the Gd-derivatized Ao α -amylase.

Differential scanning calorimetry of Ao α -amylase

Based on the initial findings regarding enzymatic activity after heat treatment, we selected two heavy atoms, Gd and Sm, for further study of thermal stabilization of Ao α -amylase. Enzymes derivatized with GdCl_3 or SmCl_3 were examined by DSC to detect differences in their thermal behavior (Fig. 1A). In the absence of heavy atoms, the denaturation temperature (T_d) for Ao α -amylase was 60.6°C . On the other hand, T_d increased to 66.8°C or 66.3°C , respectively, when a 0.2 mg/mL solution of Ao α -

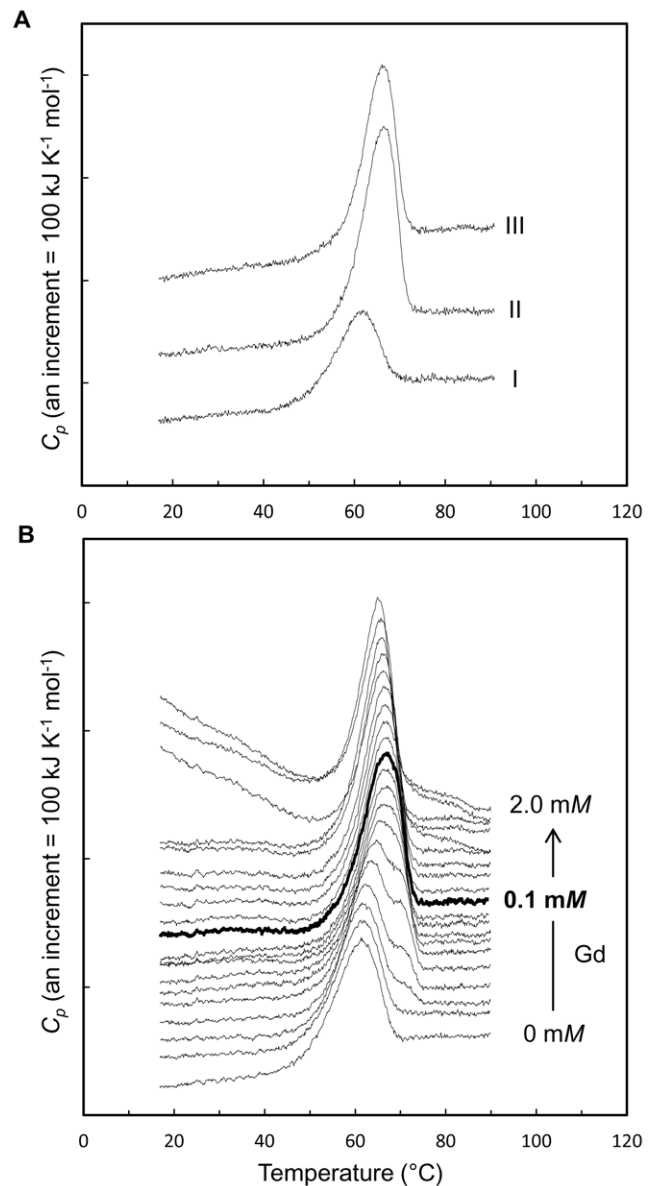


Figure 1. DSC curves of Ao α -amylase with heavy atoms at pH 5.8. (A) 0.2 mg/mL Ao α -amylase with heavy atoms. (I) no heavy atom, (II) 0.2 mM GdCl_3 , (III) 0.2 mM SmCl_3 . (B) Gd concentration dependence of the denaturation temperature of 0.4 mg/mL Ao α -amylase with $0\text{--}2.0\text{ mM}$ GdCl_3 ($0, 0.01, 0.02, 0.03, 0.04, 0.05, 0.06, 0.07, 0.08, 0.09, 0.10, 0.11, 0.12, 0.15, 0.2, 0.3, 0.5, 0.9, 1.0,$ and 2.0 mM). A concentration of 0.1 mM GdCl_3 gave the highest T_d value, 67.3°C (heavy line). The denaturation temperature, T_d , represents the temperature corresponding to the peak of the DSC curve observed at a scan rate of $200^\circ\text{C}/\text{hour}$.

doi:10.1371/journal.pone.0057432.g001

amylase was incubated with 0.2 mM of either GdCl_3 or SmCl_3 . Thus, the T_d of Ao α -amylase increased by $\sim 6^\circ\text{C}$ in the presence of these heavy atoms, indicating that the stability of the protein was remarkably improved by both ions.

We next conducted DSC experiments to evaluate the changes in stability under different concentrations ($0\text{--}2.0\text{ mM}$) of GdCl_3 , using a 0.4 mg/mL solution of Ao α -amylase (Fig. 1B, Table 1). The T_d increased with increasing Gd concentration between 0 and 0.1 mM GdCl_3 . At 0.1 mM GdCl_3 , Ao α -amylase exhibited the highest T_d value, 67.3°C ; this value is 6.3°C higher than that of the

native protein. The DSC curves show that T_d declined with increasing concentration from 0.11 to 2.0 mM $GdCl_3$, due to protein aggregation, as described below (Table 1). In the DSC measurements of the cooling and reheating processes, no excess heat capacity curve was observed in the presence or absence of Gd ions, suggesting that the heat denaturation of Ao α -amylase was irreversible under the conditions of the experiment.

Crystal structure of Gd derivatized Ao α -amylase

To elucidate the stabilization mechanism of Ao α -amylase with a T_d of 67.3°C, we determined the structures of native and Gd-derivatized proteins by X-ray crystallography. The crystal structure of the Gd-derivatized protein is shown in Fig. 2A. The structure consists of three domains: a central main domain, A (residues 1–121 and 177–380), formed by an N-terminal catalytic (β/α)₈-barrel; a small β -pleated domain, B (122–176), protruding between β 3 and α 3; and a C-terminal globular domain, C (residues 381–478), consisting of a β -structure with a Greek-key motif [26–32]. This structure is similar to previously reported X-ray structures of Ao α -amylase.

N-acetyl glucosamine (NAG)- and calcium-binding sites were present in the crystal structures of both the native and the derivatized protein (Fig. 2B and 2C). The positions of these two ligands are identical to those in the reported structure of α -amylase (PDB code: 2gvy) [32]. Since no NAG was added during the

crystallization of Ao α -amylase, this endogenous NAG may have been incorporated during the preparation steps. A calcium-binding site is located at the interface between the catalytic A domain and the B domain (Fig. 2C). This calcium ion is recognized by interactions with the side-chains of Asn121 and Asp175, the main-chain atoms of residues Glu162 and His210, and three water molecules. A characteristic feature of α -amylases is their requirement for calcium ions for activity and conformational stability [33].

In the derivatized protein structure, we found six bound Gd ions (Fig. 2A). The Gd1, Gd2, Gd3, and Gd4 ions are located in between the residues of the asymmetric chain and those of a neighboring symmetry-related chain (Fig. 3A–C). The Gd1–4 ions may act as an interchain linker, resulting in oligomerization of Ao α -amylase molecules. Gd1, Gd3, and Gd4 ions exclusively mediate interactions between the proteins, as opposed to within a single protein molecule. However, the interactions involving Gd1, Gd3, and Gd4 make no contribution to stability, because dynamic light-scattering analysis of the stabilized protein in solution suggested that it exists in a monomeric state (see below and Table 1). The position of the Gd2 ion, which interacts with both Asp233 of domain A and Glu156 of domain B, suggests that Gd2 contributes to the conformational stability of Ao α -amylase (Fig. 3A). The Gd5 ion is bound to Asp47 on the molecular surface (Fig. 3D). One Gd-binding site, Gd6, was present on the catalytic pocket of domain A (Fig. 3E). The binding of Gd6 ion to Asp206 and Glu230 was weak, with a site occupancy of 0.2. Thus, the derivatized enzyme may retain activity because of the low occupancy of the Gd6 site.

To confirm the structural changes due to derivatization, we performed a C α superposition analysis using the program *LSQKAB* [34]. The C α r.m.s.d. (root mean square deviation) between the derivative and native Ao α -amylase structures was 0.26 Å, indicating that the overall crystal structure of the derivatized protein was highly similar to the native structure. In addition, to obtain additional information regarding structural changes in solution with Gd ions, we generated near-UV circular dichroism (CD) spectra in the ranges from 250 to 320 nm (data not shown). The CD spectrum of Ao α -amylase with Gd ions was indistinguishable from that of the protein without Gd ions, further supporting that the tertiary structure of Gd-derivatized Ao α -amylase is similar to that of the native protein. From these results, we conclude that the Gd ions do not affect the overall conformation of the Ao α -amylase molecule.

In this study, it still remains unclear whether the Gd2 ion plays a significant role in stabilizing the Ao α -amylase structure. It might be difficult to specify effects of Gd ions by site-directed mutagenesis because an introduction of the point mutation in proteins affects not only the stabilizing factors of the mutation site but also those of other parts far from the substitution site [4–6]. The stabilization of Ao α -amylase was mediated by Gd ions. The ligand binding is important to the increase in thermal stability in solution [13,14]. In a study for thermal stability of tryptophan synthase, Ogasahara *et al.* have shown that the simulated interaction between the subunits with the order of $10^8 M^{-1}$ of binding constant remarkably enhances the thermal stability of the protein without conformational change [15]. The increase in T_d of Gd-binding Ao α -amylase without conformational change could be caused by the increase in the binding constant. On the other hand, covalent cross-linking in proteins by disulfide or chemical cross-linkers restrains the folding and unfolding of the protein, resulting in a decrease in the conformational entropy of the unfolded polypeptide [10–12]. Therefore, the stabilization mechanism of the Gd-binding protein is completely different from that of the cross-linked protein. Our technique using heavy atoms is

Table 1. Results of DSC and DLS experiments for 0.4 mg/mL Ao α -amylase in the presence of Gd ions at pH 5.8.

GdCl ₃ mole ratio	DSC	DLS			
		protein: Gd	T_d	peak 1	peak 2
mM	°C	molecular mass [*]	mass	molecular mass [*]	mass
		kDa	%	kDa	%
0	61.2	60.3	100		0
0.01	61.0	53.5	100		0
0.02	61.6	60.1	99.8	7099	0.2
0.03	62.4	51.4	99.5	5882	0.5
0.04	63.7	43.2	99.3	2890	0.7
0.05	64.3	40.6	98.8	6582	1.2
0.06	65.6	35.0	99.4	9821	0.6
0.07	66.6	45.6	98.9	9588	1.1
0.08	66.9	56.2	98.9	2.3×10 ⁴	1.1
0.09	66.9	40.9	99.2	2.6×10 ⁴	0.8
0.10	67.3	42.8	99.3	3.3×10 ⁴	0.7
0.11	66.6	46.0	98.6	4.2×10 ⁴	1.4
0.12	66.8		0	3.6×10 ⁴	100
0.15	66.7		0	5.0×10 ⁴	100
0.20	66.9		0	1.8×10 ⁵	100
0.30	66.4		0	3.0×10 ⁵	100
0.50	66.2		0	10 ⁶	100
0.90	65.9		0	10 ⁶	100
1.00	65.6		0	10 ⁶	100
2.00	65.1		0	10 ⁶	100

*molecular mass estimated from the measured radius (*DYNAMICS*, Protein Solutions).

A maximum T_d is observed at a concentration of 0.1 mM $GdCl_3$ (bold).

doi:10.1371/journal.pone.0057432.t001

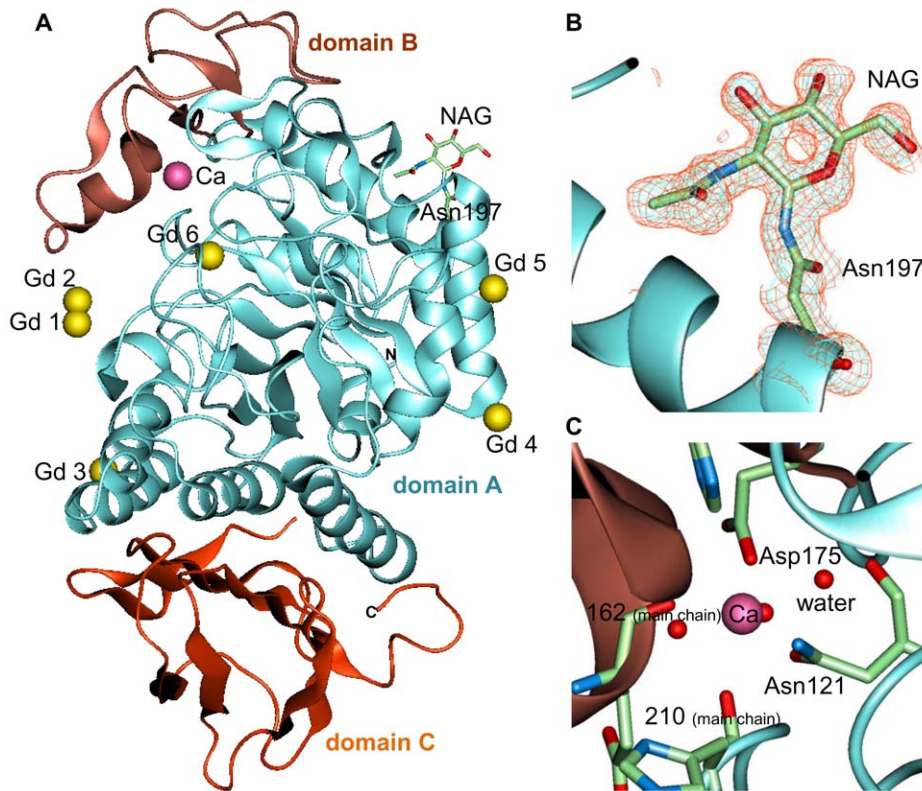


Figure 2. The crystal structure of Gd-derivatized Ao α -amylase. (A) Overall structure shown in ribbon diagram. The three domains, A, B, and C, are colored light blue, brown, and orange, respectively. NAG molecule and residue Asn197 are depicted as licorice models. Bound Ca and Gd ions are depicted as pink and yellow spheres, respectively. Close-up view of (B) NAG binding site with $(2Fo-Fc)$ electron-density map contoured at 1.2σ (blue mesh) and 0.6σ (orange mesh) level and (C) Ca binding site. The residues are depicted as licorice models. The perspective is the same as that in Fig. 2A. Drawn in QUANTA2000.

doi:10.1371/journal.pone.0057432.g002

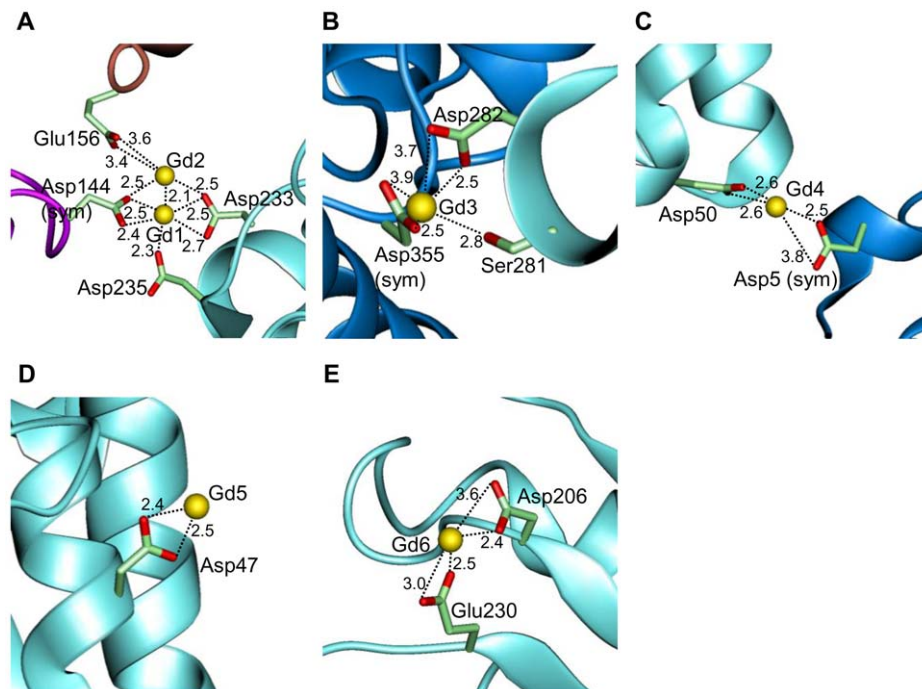


Figure 3. Close-up view of Gd binding sites. (A–E) Bound Gd ions and the interacting residues are depicted as yellow spheres and licorice models, respectively. The neighboring symmetry-related chains of domain A and B are colored blue and purple, respectively. The perspective is the same as that in Fig. 2A. Drawn in QUANTA2000.

doi:10.1371/journal.pone.0057432.g003

one of those methods for thermal stabilization of proteins, suggesting that the application of a variety of techniques is essential to eliminate the time consuming procedure during the trial and error process.

Dynamic light-scattering (DLS) experiment

A DLS experiment revealed that Ao α -amylase exists in a monomeric state in the absence of Gd ions (Table 1). However, the monomeric state shifted toward the oligomeric state upon addition of Gd ions. For GdCl₃ concentrations between 0.02 and 0.11 mM, bimodal peaks were observed (98.6–99.8% mass in the monomeric state and 0.2–1.4% mass in the oligomeric state). For Gd concentrations between 0.12 and 2.0 mM, a bimodal analysis revealed an estimated molecular mass of 10⁴–10⁶ kDa, suggesting aggregation of Ao α -amylase in solution. Thus, the inclusion of excess Gd ions actually appears to promote the aggregation of this enzyme.

At 0.1 mM GdCl₃, i.e., the condition that confers maximum T_d , 99% of the protein is in the monomeric state (Table 1), indicating that the Gd ions in the monomeric crystal structure (Fig. 3) contribute predominantly to the stabilization of this protein. The Gd ion concentrations associated with protein aggregation correspond to the concentrations at which the T_d decreases. The formation of aggregates might be due to Gd ions acting as inter-chain linkers (Gd1, 3, 4 in Fig. 3). Although the addition of excess Gd ions negatively affects the stability of this protein, the T_d in the aggregated state under in 2.0 mM GdCl₃ is still approximately 4°C higher than that of the native protein. These results indicate that the stability of Ao α -amylase does not deteriorate significantly upon aggregation. In the crystal structure, one molecule of α -amylase binds to six Gd ions. However, the maximum T_d is observed at a 1:13 molar ratio of protein to Gd (Table 1), implying that Gd ions interact with Ao α -amylase in the equilibrium state with weak binding constants.

In summary, we examined the applicability of heavy-atom derivatization as a stabilization technique, using Ao α -amylase protein in the presence of lanthanide ions. The T_d of Ao α -amylase increased in the presence of Gd ion, up to a maximum at 0.1 mM GdCl₃, and decreased relative to this maximum at higher concentrations. At the maximum, the T_d value of the Gd-derivatized protein was 6°C higher than that of the native protein. The stabilization mechanism of the enzyme by Gd was elucidated by analysis of crystal structure solved at 1.5 Å resolution, and by observation of its physicochemical properties (such as changes in T_d) and its oligomeric state in solution. The results suggest that the bound heavy atoms contribute substantially to the thermal stability of this enzyme. A similar stabilization by the heavy-atom derivatization technique, using ions selected by the HATODAS software, has been observed in a putative α -ribazole-5'-phosphate phosphatase from *Thermus thermophilus* HB8. The T_d of that protein in the presence of Pt ions was 95.6°C, 16.4°C higher than that of the native protein (Sugahara *et al.*, in preparation).

The results presented here confirm that HATODAS is a powerful tool for identifying heavy atoms for use in stabilization of two examined proteins, and suggest that the derivatization technique is useful for rapid and effective stabilization of proteins. One clear advantage of the heavy-atom derivatization technique is its simplicity: all that is required is the addition of heavy atoms to protein solutions. This method may, therefore, be applicable to a wide range of proteins.

Materials and Methods

Heavy-atom selection for thermostabilization

As a test protein for this work, we used commercially available α -amylase (endo-1,4- α -D-glucan glucohydrolase) from *Aspergillus oryzae* (EC 3.2.1.1, MW = 52.4 × 10³, Sigma, Cat. No. 10065) without further purification. The optimal conditions for α -amylase in industrial application are pH and no Ca²⁺ [35,36]. The program HATODAS (<http://hatodas.harima.riken.jp/>) identified six candidate heavy atoms based on the amino-acid sequence of Ao α -amylase and pH 5.8 as the query terms. Ao α -amylase activity with the selected heavy atoms was examined using the starch-iodine assay method [37]. A 0.1 mL aliquot of Ao α -amylase at 0.4 mg/mL in 0.1 M MES-NaOH (pH 5.8) with 1.0 mM heavy atoms was incubated for 5 min at 70°C in a water bath; this temperature was chosen because T_d for Ao α -amylase is 61°C in the absence of heavy atoms. The reactions were initiated by adding 0.1 mL of 0.25% (*w/v*) starch solution as a substrate to α -amylase solutions at 20°C. The α -amylase activity was confirmed by adding 0.1 mL of iodine reagent [0.02% (*w/v*) I₂, 0.2% (*w/v*) KI] to 0.2 mL of the protein-starch solution at 20°C.

Differential scanning calorimetry (DSC)

DSC experiments were performed at scan rate of 200°C/hour using a VP-capillary DSC platform. For the measurements of Sm and Gd ions, the protein concentration was 0.2 mg/mL in 50 mM MES-NaOH (pH 5.8), containing 0.2 mM SmCl₃ or 0.2 mM GdCl₃. For the measurements of heavy-atom concentration dependence, the protein concentration was 0.4 mg/mL in 50 mM MES-NaOH buffer (pH 5.8) containing 0.01, 0.02, 0.03, 0.04, 0.05, 0.06, 0.07, 0.08, 0.09, 0.10, 0.11, 0.12, 0.15, 0.2, 0.3, 0.5, 0.9, 1.0, or 2.0 mM GdCl₃. All samples were dialyzed overnight at 4°C against buffer without heavy atoms and then filtered through a membrane with 0.22 μ m pores. DSC data were analyzed using the Origin software supplied with the instrument (MicroCal Inc.). Molar excess heat capacities (C_p) were obtained by normalizing against the Ao α -amylase concentration and the volume of the calorimeter cell. Apparent denaturation temperature (T_d) value was defined as the temperature associated with maximum C_p .

Crystallization and diffraction data collection

Diffraction-quality crystals of Ao α -amylase were obtained using the oil microbatch method [38] on the Autolabo automatic crystallization system [39]. A crystallization drop of 1.0 μ L, in the presence of synthetic zeolite molecular sieves as heteroepitaxial nucleants [40,41], was created by mixing 1:1 mixture of 28.0 mg/mL protein solution in 0.02 M MES-NaOH (pH 5.8) and precipitant solution composed of 40% (*w/v*) polyethylene glycol (PEG) 8,000, 0.2 M CaCl₂, and 0.1 M MES-NaOH (pH 5.8) in a well of a Nunc HLA crystallization plate (Nalge Nunc International) which was then covered with 20 μ L of paraffin oil. The resulting Ao α -amylase crystals were submitted to a heavy-atom derivatization experiment. The Gd derivative was prepared by soaking native crystals with 10 mM GdCl₃, 40% (*w/v*) PEG 8,000, 0.2 M CaCl₂, 0.1 M MES-NaOH (pH 5.8). Although the SmCl₃ derivatization was attempted using concentrations in the range 0.1–10 mM, this treatment caused the crystals to crack, and structure determination was therefore impossible.

All crystals were directly mounted in a cryoloop from the crystallization drop and flash-cooled at 100 K in a nitrogen gas stream. Complete diffraction data sets were collected using an in-house Rigaku R-Axis VII image-plate detector with Cu $K\alpha$ radiation and a Rigaku R-Axis V image-plate detector with

synchrotron radiation at BL26B1 of SPring-8, Japan [42]. All data were processed using the program *HKL-2000* [43].

Structure determination

Positioning of one Ao α -amylase molecule in the asymmetric unit was accomplished using the molecular-replacement method as implemented in the program *MOLREP* [44], based on the crystal structure deposited in the Protein Data Bank (PDB code 2taa). The structure of the Gd-bound protein was isomorphous to that of the native form and was determined by difference Fourier analysis using the corresponding model of the native structure. Manual model revision was performed using *QUANTA2000* software (Accelrys Inc.).

Bound ions were observed in the structure of the Gd-soaked crystal. Based on comparison of temperature factors to those of neighboring atoms, and from their coordination with ion-binding residues, the bound ions are most likely to be Gd ions from the heavy-atom soaking reagent. This interpretation is in agreement with the fact that strong signals are observed at the ion sites in the anomalous Fourier map at a wavelength of 1.000 Å, prepared using the program *FFT* in CCP4 suite [45].

The program *CNS* [46] was used for structure refinement and electron-density map calculation. Each cycle of refinement with bulk solvent and overall anisotropic B-factor corrections consisted of rigid-body refinement, simulated annealing incorporating the slow-cool protocol, positional refinement, and B-factor refinement (individual or group). Several cycles of model revision and refinement yielded the final models. The stereochemical quality of the final structures was verified using the program *PROCHECK* [47]. Statistics of the data collection and refinement are shown in Table 2. The structural data are available in the Protein Data Bank under the accession numbers 3VX0, 3VX1.

Dynamic light-scattering study

Ao α -amylase was examined by dynamic light-scattering experiment using a DynaPro MS/X (Protein Solutions) instrument at a protein concentration of 0.4 mg/mL in 50 mM MES-NaOH (pH 5.8) containing 0–2.0 mM GdCl₃. Several measurements were taken at 293 K and analyzed using the program *DYNAMICS* v.5.26.60 (Protein Solutions). The average values of two measurements of mass at each GdCl₃ concentration are shown in Table 1.

CD spectra

Circular dichroism (CD) spectra of Ao α -amylase were recorded on a Jasco J-725 spectropolarimeter (Jasco Co., Japan). Near-UV CD spectra in the wavelength range from 250 to 320 nm were scanned 16 times at a scan rate of 20 nm/min, using a time constant of 0.25 sec. The light-path length of the cell was 10 mm in the near-UV region. For the measurements at 25°C, the protein concentrations were 0.75 mg/mL in 50 mM MES-NaOH (pH 5.8) with 0.04 mM or 0.2 mM GdCl₃.

References

- Kirk O, Borchert TV, Fuglsang CC (2002) Industrial enzyme applications. *Current Opinion in Biotechnology* 13: 345–351.
- Lehmann M, Wyss M (2001) Engineering proteins for thermostability: the use of sequence alignments versus rational design and directed evolution. *Current Opinion in Biotechnology* 12: 371–375.
- Cherry JR, Fidantset AL (2003) Directed evolution of industrial enzymes: an update. *Current Opinion in Biotechnology* 14: 438–443.
- Yutani K, Ogasahara K, Tsujita T, Sugino Y (1987) Dependence of conformational stability on hydrophobicity of the amino acid residue in a series of variant proteins substituted at a unique position of tryptophan synthase alpha subunit. *Proc Natl Acad Sci U S A* 84: 4441–4444.
- Takano K, Yamagata Y, Fujii S, Yutani K (1997) Contribution of the hydrophobic effect to the stability of human lysozyme: calorimetric studies and

Table 2. Data-collection and refinement statistics.

Protein	Native	Gd derivative
No. of ligands		
NAG	1	1
Ca ion	1	1
Gd ion		6
Space group	<i>P</i> 2 ₁ 2 ₁ 2 ₁	<i>P</i> 2 ₁ 2 ₁ 2 ₁
Unit-cell parameter		
<i>a</i> (Å)	50.37	48.52
<i>b</i> (Å)	66.68	65.62
<i>c</i> (Å)	131.55	130.24
Wavelength (Å)	1.54	1.000
Resolution range (Å)	20–2.2 (2.28–2.20)	20–1.50 (1.55–1.50)
No. of unique reflections	23047 (2192)	66313 (6332)
Redundancy	6.6 (6.3)	5.7 (5.4)
Completeness (%)	98.6 (96.1)	98.5 (95.3)
$R_{\text{merge}}^{\dagger}$ (%)	8.3 (33.6)	10.6 (54.1)
$\langle I/\sigma(I) \rangle$	9.4 (5.6)	7.7 (3.6)
mosaicity (°)	0.77–0.86	0.46–0.65
Refinement		
Resolution range (Å)	20–2.2	20–1.50
$R_{\text{cryst}}/R_{\text{free}}^{\S}$	20.8/24.6	19.2/19.9
No. of molecules in ASU	1	1
Rms deviation		
Bond length (Å)	0.009	0.009
Bond angle (°)	1.5	1.5
PDB code	3vx1	3vx0

Values in parentheses are for the outermost shell.

$\dagger R_{\text{merge}} = \sum_{hkl} \sum_i |I_i(hkl) - \langle I(hkl) \rangle| / \sum_{hkl} \sum_i I_i(hkl)$, where $I_i(hkl)$ is the i th observation of reflection hkl and $\langle I(hkl) \rangle$ is the weighted average intensity for all observations i of reflection hkl .

$\S R_{\text{cryst}} = \sum_{hkl} ||F_{\text{obs}}| - |F_{\text{calc}}|| / \sum_{hkl} |F_{\text{obs}}|$, where $|F_{\text{obs}}|$ and $|F_{\text{calc}}|$ are the observed and calculated structure-factor amplitudes, respectively. R_{free} was calculated with 5% of the reflections chosen at random and omitted from refinement. doi:10.1371/journal.pone.0057432.t002

Acknowledgments

We thank the beamline staff for assistance during data collection at BL26B1 of SPring-8 (proposal No. 20110101).

Author Contributions

Revisions of final manuscript: KY. Conceived and designed the experiments: MS KY. Performed the experiments: MS MT. Analyzed the data: MS KY. Wrote the paper: MS.

X-ray structural analyses of the nine valine to alanine mutants. *Biochemistry* 36: 688–698.

- Funahashi J, Takano K, Yutani K (2001) Are the parameters of various stabilization factors estimated from mutant human lysozymes compatible with other proteins? *Protein Eng* 14: 127–134.
- Wold F (1972) Bifunctional reagents. *Methods Enzymol* 25: 623–651.
- Peters K, Richards FM (1977) Chemical cross-linking: reagents and problems in studies of membrane structure. *Annu Rev Biochem* 46: 523–551.
- Wong SS, Wong LJC (1992) Chemical crosslinking and the stabilization of proteins and enzymes. *Enzyme Microb Technol* 14: 866–874.
- Pantoliano MW, Ladner RC, Bryan PN, Rollence ML, Wood JF, et al. (1987) Protein engineering of subtilisin BPN': enhanced stabilization through the

- introduction of two cysteines to form a disulfide bond. *Biochemistry* 26: 2077–2082.
11. Pace CN, Grimsley GR, Thomson JA, Barnett BJ (1988) Conformational stability and activity of ribonuclease T1 with zero, one, and two intact disulfide bonds. *J Biol Chem* 263: 11820–11825.
 12. Matsumura M, Signor G, Matthews BW (1989) Substantial increase of protein stability by multiple disulphide bonds. *Nature* 342: 291–293.
 13. Schellman JA (1975) Macromolecular binding. *Biopolymers* 14: 999–1018.
 14. Schellman JA (1976) The effect of binding on the melting temperature of biopolymers. *Biopolymers* 15: 999–1000.
 15. Ogasahara K, Ishida M, Yutani K (2003) Stimulated interaction between α and β subunits of tryptophan synthase from hyperthermophile enhances its thermal stability. *J Biol Chem* 278: 8922–8928.
 16. Donovan JW, Ross KD (1975) Nonequivalence of the metal binding sites of conalbumin. Calorimetric and spectrophotometric studies of aluminum binding. *J Biol Chem* 250: 6022–6025.
 17. Kuroki R, Kawakita S, Nakamura H, Yutani K (1992) Entropic stabilization of a mutant human lysozyme induced by calcium binding. *Proc Natl Acad Sci U S A* 89: 6803–6807.
 18. Vepintsev DB, Narayan M, Permyakov SE, Uversky VN, Brooks CL, et al. (1999) Fine tuning the N-terminus of a calcium binding protein: alpha-lactalbumin. *Proteins* 37: 65–72.
 19. Vieille C, Zeikus GJ (2001) Hyperthermophilic enzymes: sources, uses, and molecular mechanisms for thermostability. *Microbiol Mol Biol Rev* 65: 1–43.
 20. Xue Y, Wang S, Feng X (2009) Effect of metal ion on the structural stability of tumour suppressor protein p53 DNA-binding domain. *J Biochem* 146: 193–200.
 21. Jayakanthan J, Takada K, Sawano M, Ogasahara K, Mizutani H, et al. (2009) Crystal structural and functional analysis of the putative dipeptidase from *Pyrococcus horikoshii* OT3. *J Biophys* 434038.
 22. Blundell TL, Johnson LN (1976) *Protein Crystallography*. London: Academic Press. pp. 183–239.
 23. Ericsson UB, Hallberg BM, Detitta GT, Dekker N, Nordlund P (2006) Thermofluor-based high-throughput stability optimization of proteins for structural studies. *Anal Biochem* 357: 289–298.
 24. Sugahara M, Asada Y, Ayama H, Ukawa H, Taka H, et al. (2005) Heavy-atom Database System: a tool for the preparation of heavy-atom derivatives of protein crystals based on amino-acid sequence and crystallization conditions. *Acta Crystallogr D Biol Crystallogr* 61: 1302–1305.
 25. Sugahara M, Asada Y, Shimada H, Taka H, Kunishima N (2009) HATODAS II—heavy-atom database system with potentiality scoring. *J Appl Crystallogr* 42: 540–544.
 26. Akabori S, Ikenaka T, Hagihara B (1954) Isolation of crystalline taka-amylase A from ‘Takadiastase Sankyō’. *J Biochem* 41: 577–582.
 27. Matsuura Y, Kusunoki M, Date W, Harada S, Bando S, et al. (1979) Low resolution crystal structures of Taka-amylase A and its complexes with inhibitors. *J Biochem* 86: 1773–1783.
 28. Matsuura Y, Kusunoki M, Harada W, Tanaka N, Iga Y, et al. (1980) Molecular structure of Taka-amylase A. I. Backbone chain folding at 3 Å resolution. *J Biochem* 87: 1555–1558.
 29. Matsuura Y, Kusunoki M, Harada W, Kakudo M (1984) Structure and possible catalytic residues of Taka-amylase A. *J Biochem* 95: 697–702.
 30. Swift HJ, Brady L, Derewenda ZS, Dodson EJ, Dodson GG, et al. (1991) Structure and molecular model refinement of *Aspergillus oryzae* (TAKA) α -amylase: an application of the simulated-annealing method. *Acta Crystallogr B Structural Science* 47: 535–544.
 31. Brzozowski AM, Davies GJ (1997) Structure of the *Aspergillus oryzae* α -amylase complexed with the inhibitor acarbose at 2.0 Å resolution. *Biochemistry* 36: 10837–10845.
 32. Vujčić-Žagara A, Dijkstra BW (2006) Monoclinic crystal form of *Aspergillus niger* α -amylase in complex with maltose at 1.8 Å resolution. *Acta Crystallogr. F Structural Biology and Crystallization Communications* 62: 716–721.
 33. Tripathi P, Hofmann H, Kayastha AM, Ulbrich-Hofmann R (2008) Conformational stability and integrity of α -amylase from mung beans: Evidence of kinetic intermediate in GdmCl-induced unfolding. *Biophysical Chemistry* 137: 95–99.
 34. Kabsch W (1976) A solution for the best rotation to relate two sets of vectors. *Acta Crystallogr A Foundations of Crystallography* 32: 922–923.
 35. Chang CT, Tang MS, Lin CF (1995) Purification and properties of alpha-amylase from *Aspergillus oryzae* ATCC 76080. *Biochem Mol Biol Int* 36: 185–193.
 36. Richardson TH, Tan X, Frey G, Callen W, Cabell M, et al. (2002) A novel, high performance enzyme for starch liquefaction: discovery and optimization of a low pH, thermostable α -amylase. *J Biol Chem* 277: 26501–26507.
 37. Xiao ZZ, Storms R, Tsang A (2006) A quantitative starch-iodine method for measuring alpha-amylase and glucoamylase activities. *Anal Biochem* 351: 146–148.
 38. Chayen NE, Shaw Stewart PD, Maeder DL, Blow DM (1990) An automated system for microbatch protein crystallisation and screening. *J Appl Crystallogr* 23: 297–302.
 39. Sugahara M, Shimizu K, Asada Y, Fukunishi H, Kodera H, et al. (2010) Autolabo: an automated system for ligand-soaking experiments with protein crystals. *J Appl Crystallogr* 43: 940–944.
 40. Sugahara M, Asada Y, Morikawa Y, Kageyama Y, Kunishima N (2008) Nucleant-mediated protein crystallization with the application of microporous synthetic zeolite. *Acta Crystallogr D Biol Crystallogr* 64: 686–695.
 41. Sugahara M, Kageyama-Morikawa Y, Kunishima N (2011) Packing space expansion of protein crystallization screening with synthetic zeolite as a heteroepitaxial nucleant. *Crystal Growth & Design* 11: 110–120.
 42. Ueno G, Kanda H, Hirose R, Ida K, Kumasaka T, et al. (2006) RIKEN structural genomics beamlines at the SPring-8; high throughput protein crystallography with automated beamline operation. *J Struct Funct Genomics* 7: 15–22.
 43. Otwinowski Z, Minor W (1997) Processing of X-ray diffraction data collected in oscillation mode. *Methods Enzymol* 276: 307–326.
 44. Vagin A, Teplyakov A (1997) MOLREP: an automated program for molecular replacement. *J Appl Crystallogr* 30: 1022–1025.
 45. Collaborative Computational Project, Number 4 (1994) The CCP4 suite: programs for protein crystallography. *Acta Crystallogr D Biol Crystallogr* 50: 760–763.
 46. Brünger AT, Adams PD, Clore GM, DeLano WL, Gros P, et al. (1998) Crystallography and NMR system: a new software suite for macromolecular structure determination. *Acta Crystallogr D Biol Crystallogr* 54: 905–921.
 47. Laskowski RA, MacArthur MW, Moss DS, Thornton JM (1993) PROCHECK: a program to check the stereochemical quality of protein structures. *J Appl Crystallogr* 26: 283–291.